Macromolecules
A R T I C L E

Scale-Dependent Electrostatic Stiffening in Biopolymers

Alexander Gubarev,[†,‡] **Jan-Michael Y. Carrillo,**[†] **and Andrey V. Dobrynin**[*,†]

[†]*Polymer Program, Institute of Materials Science, Department of Physics, University of Connecticut, Storrs, Connecticut 06269-3136, and* [‡]*Department of Physics, Saint-Petersburg State University, Saint-Petersburg, Russia*

ABSTRACT: Using a combination of the molecular dynamics simulations and theoretical calculations, we have demonstrated that bending rigidity of biological polyelectrolytes (semiflexible charged polymers) is scale-dependent. A bond−bond correlation function describing a chain's orientational memory can be approximated by a sum of two exponential functions manifesting the existence of the two characteristic length scales. One describes the chain's bending rigidity at the distances along the polymer backbone shorter than the Debye screening length, whereas another controls the long-scale chain's orientational correlations. The short-length scale bending rigidity is proportional to the Debye screening length at high salt concentrations and shows a weak logarithmic dependence on salt concentration when the Debye screening length exceeds a crossover value of $\kappa_{cr}^{-1} \propto (l_B \alpha^2 / l_p)^{-1/2}$ (where l_B is the Bjerrum length, α is the fraction of ionized groups, and l_p is a bare persistence length). The long-scale chain's bending rigidity has a well-known Odijk−Skolnick−Fixman form with a quadratic dependence on the Debye radius. Simulation results and a theoretical model demonstrate good qualitative agreement.

1. Introduction

Electrostatic interactions play an important role in controlling properties of biological objects, such as DNA, F-actin, microtubules and filamentous viruses.[1−3] The change in the ionic environment is known to influence the conformational properties of DNA significantly. Condensation of multivalent ions triggers an abrupt collapse of T4 phage DNA from coil-like conformations to compact structure inside the viral capsid.[1] The decrease in the volume of the DNA molecule could be significant and reaches the volume compression ratio of 6900 times.[1] The force−elongation measurements,[4] diffusion coefficient measurements,[5] and studies of the effect of confinement of the λ-DNA[6] show that with increasing solution ionic strength, the chain stiffness decreases. The ability to manipulate molecular properties, such as the chain's bending energy, by controlling its environment was utilized in DNA separation[7] and gene mapping[8] and is at the heart of the future of nanotechnology.

The concept of the electrostatic persistence length of semiflexible polyelectrolytes was introduced by Odijk[9] and by Skolnick and Fixman[10] (OSF). They studied bending rigidity of a semiflexible polyelectrolyte chain with ionic groups interacting via the screened Debye−Huckel potential. This is a crude model of DNA in salt solutions where electrostatic interactions are exponentially screened by salt ions on the length scales larger than the Debye screening length, κ^{-1}. However, despite the exponential decay of the strength of the electrostatic interactions, the covalent bonding of ionic groups into the polymer chains extends their range beyond the Debye screening length, leading to strong orientational correlations between chain segments. A bond orientational memory propagates far beyond the Debye screening length, κ^{-1}, inducing extra chain stiffening, which is proportional to the square of the Debye radius. The OSF theory has been challenged. Different authors have shown that the electrostatic part of the

chain's bending energy scales linearly with the Debye radius. (For a recent overview of the subject, see refs 11−14).

In this article, we present a new model of the electrostatic induced rigidity of biological (semiflexible) polyelectrolytes by extending the idea of a scale dependence of the chain's persistence length developed in refs 11, 15, and 16. We will show that the electrostatic-induced stiffening of a semiflexible polyelectrolyte is a multiscale process that can be approximated by two characteristic length scales. One describes the decay of the bond−bond orientational memory at the distances along the polymer backbone shorter than the Debye screening length, whereas another controls long-scale orientational correlations. At high salt concentrations, when intrachain electrostatic interactions are significantly screened, the short-length scale correlation length (bending rigidity) is proportional to the Debye screening length, whereas the long-scale correlation length is proportional to the square of the Debye radius.[9,10] However, when the Debye screening length exceeds a crossover value, the short-length scale correlation length has a weak logarithmic dependence on the Debye screening length. Note that a logarithmic dependence of the chain's orientational correlations is a characteristic feature of a semiflexible chain under tension generated by local electrostatic interactions. A crossover shifts toward larger values of the Debye screening lengths with increasing bare chain persistence length.

The rest of the article is organized as follows. In Section 2, we present the results of the molecular dynamics simulations of semiflexible polyelectrolyte chains. Section 3 discusses the results of the high-temperature expansion and variational calculations. At the end of the section, we compare derived scaling relations with simulation results. Finally, Section 4 summarizes our results and discusses the possibility of an experimental verification of our findings.

2. Model and Simulation Results

To elucidate the factors controlling the electrostatic-induced chain's stiffening of biopolymers, we have performed molecular

*Corresponding author. E-mail: avd@ims.uconn.edu.

dynamics simulations[17] of semiflexible polyelectrolyte chains. A polyelectrolyte chain was modeled by a bead−spring chain of charged particles with diameter σ and consisting of $N_m = 200$ beads (monomers). The connectivity of the monomers into a polymer chain was maintained by the finite extension nonlinear elastic (FENE) potential

$$U_{FENE}(r) = -0.5 k_{spring} R_{max}^2 \ln\left(1 - \frac{r^2}{R_{max}^2}\right) \quad (1)$$

where k_{spring} is the spring constant set to be $k_{spring} = 30 k_B T/\sigma^2$ and $k_{spring} = 90 k_B T/\sigma^2$ for the systems with the larger value of the electrostatic coupling constant ($A_{el} = 100$; see discussion below), the maximum bond length is $R_{max} = 1.5\sigma$, k_B is the Boltzmann constant, and T is the absolute temperature. The repulsive part of the bond potential was modeled by the Lennard-Jones potential with a value of the Lennard-Jones interaction parameter $\varepsilon_{LJ} = 0.34 k_B T$. The chain bending rigidity was introduced into the model through a bending potential controlling the mutual orientations between two neighboring along the polymer backbone unit bond vectors $\vec{n}_i$ and $\vec{n}_{i+1}$

$$U_{i,i+1}^{bend} = k_B T K (1 - (\vec{n}_i \cdot \vec{n}_{i+1})) \quad (2)$$

In our simulations the value of the bending constant, K, was varied between 25 and 160. Note that the chain persistence length, l_p, is proportional to the bending constant, $l_p = bK$, where b is the bond length.

Electrostatic interactions between charged monomers on the polymer backbone separated by a distance r_{ij} were taken into account on the level of the screened Coulomb potential

$$U_{Coul}(r_{ij}) = k_B T \frac{A_{el}\sigma}{r_{ij}} \exp(-\kappa r_{ij}) \quad (3)$$

where the parameter $A_{el} = e^2\alpha^2/\varepsilon k_B T\sigma$ describes the strength of the electrostatic interactions between charged monomers carrying an effective charge αe in a medium with the dielectric constant, ε, in terms of the thermal energy, $k_B T$. In our simulations, we have assumed that a polyelectrolyte chain is uniformly charged. The Debye screening length, κ^{-1}, depends on the parameters of the system as $\kappa^2 = 8\pi l_B c_s$, where $l_B = e^2/\varepsilon k_B T$ is the Bjerrum length and c_s is the salt concentration.

The simulations were performed at a constant temperature, which was maintained by coupling the system to the Langevin thermostat.[17] In this case, the motion of monomers is described by the following equations

$$m\frac{d\vec{v}_i(t)}{dt} = \vec{F}_i(t) - \xi\vec{v}_i(t) + \vec{F}_i^R(t) \quad (4)$$

where m is the bead mass, $\vec{v}_i(t)$ is the bead velocity, and $\vec{F}_i(t)$ denotes the net deterministic force acting on the ith bead. The stochastic force $\vec{F}_i^R(t)$ has a zero average value $\langle \vec{F}_i^R(t) \rangle = 0$ and δ-functional correlations $\langle \vec{F}_i^R(t)\vec{F}_i^R(t') \rangle = 6k_B T\xi\delta(t - t')$. The friction coefficient, ξ, was set to $\xi = m/\tau_{LJ}$, where τ_{LJ} is the standard LJ-time $\tau_{LJ} = \sigma(m/k_B T)^{1/2}$. The velocity Verlet algorithm with a time step of $\Delta t = 0.01\tau_{LJ}$ was used for the integration of the equations of motion, eq 4. Simulations were performed using the following procedure: at the beginning of each simulation run, a polyelectrolyte chain in a self-avoiding walk configuration was placed in the center of the simulation box. The system was pre-equilibrated for 2×10^7 MD steps. This was followed by a production run lasting 2×10^8 MD steps. Such long simulation runs were required to obtain a good averaging of the bond−bond
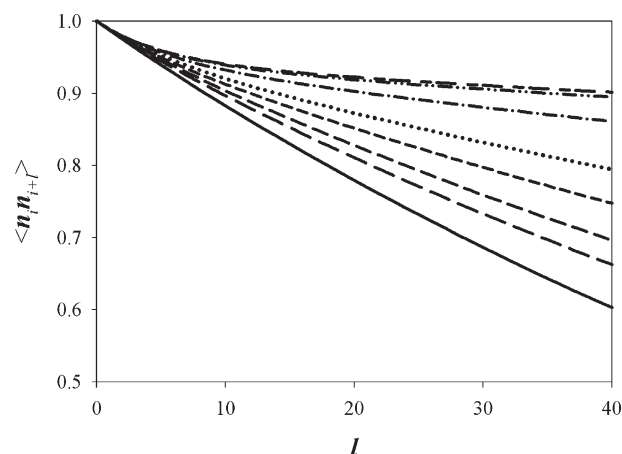

Figure 1. Bond−bond correlation functions of semiflexible polyelectrolyte chains with the degree of polymerization, $N_m = 200$, electrostatic coupling constant, $A_{el} = 1.0$, bending constant, $K = 80.0$, and different values of the Debye screening length, $\kappa\sigma = 1/7$ (long dashed line), $\kappa\sigma = 0.1$ (medium dashed line), $\kappa\sigma = 0.07$ (short dashed line), $\kappa\sigma = 0.05$ (dotted line), $\kappa\sigma = 0.025$ (dashed−dotted line), $\kappa\sigma = 0.01$ (dashed−dotted−dotted line), and $\kappa\sigma = 0.005$ (long−short dashed line). The bond−bond correlation function of a neutral chain is shown by a solid line.

correlation function at large separations along the polymer backbone. Note that relatively short chains in our simulations were selected to minimize the chain's swelling effects on the bond−bond orientational correlations.

The analysis of the effect of the Debye screening length, the initial chain bending rigidity, K, and the strength of the electrostatic interactions, A_{el}, on the effective chain bending rigidity was done by monitoring the evolution of the bond−bond correlation function, $\langle \vec{n}_i \cdot \vec{n}_j \rangle$. Figure 1 shows the dependence of the shape of the correlation function on the Debye screening length for the system with $K = 80$ and $A_{el} = 1$. To minimize the end effects in obtaining the average values of the bond−bond correlation functions, we have considered only 100 bonds in the middle of the chain during the averaging procedure. Our simulations show that this correlation function has two different functional forms. For small values of the Debye screening length, $\kappa^{-1} < 6\sigma$, the bond−bond correlations are well described by a single exponential function

$$\langle (\vec{n}_i \cdot \vec{n}_{i+l}) \rangle = \exp(-|l|/\lambda) \quad (5)$$

However, above a threshold value of the Debye screening length, $\kappa^{-1} > 6\sigma$, our simulation data can be fitted only by a combination of two exponential functions

$$\langle (\vec{n}_i \cdot \vec{n}_{i+l}) \rangle = (1 - \beta)\exp\left(-\frac{|l|}{\lambda_1}\right) + \beta\exp\left(-\frac{|l|}{\lambda_2}\right) \quad (6a)$$

This form of the bond−bond correlation function indicates that above a threshold value of the Debye screening length, there are two different length scales that describe bending rigidity of a polyelectrolyte chain. The values of the parameters λ and λ_1 are always large such that we can expand eq 6a in the power series of l/λ_1. This results in the following modification of 6a

$$\langle (\vec{n}_i \cdot \vec{n}_{i+l}) \rangle \approx 1 - (1 - \beta)\frac{|l|}{\lambda_1} + \beta\left(\exp\left(-\frac{|l|}{\lambda_2}\right) - 1\right) \quad (6b)$$
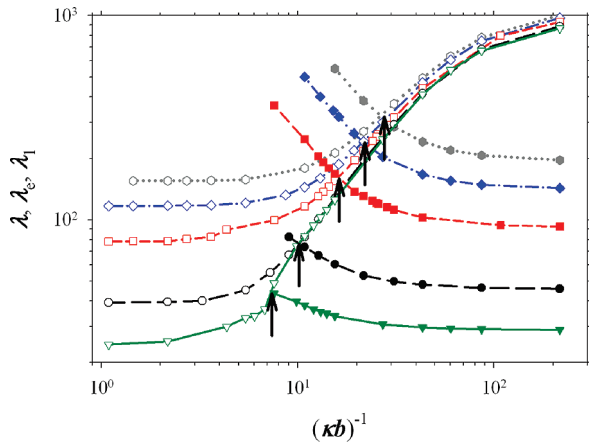
Figure 2. Dependence of the bending rigidities λ, λ_e, and λ_1 on the Debye screening length for semiflexible polyelectrolyte chains with the degree of polymerization, $N_m = 200$, electrostatic coupling constant, $A_{el} = 1.0$, and with different bending constants, $K = 25.0$ (green solid line with inverted triangles), $K = 40.0$ (long-dashed line with circles), $K = 80.0$ (red short dashed line with squares), $K = 120.0$ (blue dashed−dotted line with rhombs), and $K = 160.0$ (gray dotted line with hexagons). Arrows show intersection points between λ_1 and λ_e.

Note that the second term in the right-hand side (rhs) of this equation has a form characteristic of a semiflexible chain under tension.[18] We can introduce an effective chain bending constant, λ_e, and effective force, f_e, by setting $(\lambda_e/f_e)^{1/2} = \lambda_2$ and $(\lambda_e f_e)^{1/2} = \beta^{-1}$. Therefore, the effective chain bending rigidity is equal to $\lambda_e = \lambda_2/\beta$, and the effective force is $f_e = 1/\lambda_2\beta$.

In Figure 2, we have plotted the dependence of the chain's dimensionless bending rigidities λ, λ_1, and λ_e on the Debye screening length. As one can see from the plot, the value of the chain's bending constant, λ_e, increases as the value of the Debye screening length decreases. However, the long-length scale bending rigidity, λ_1, increases with increasing value of the Debye radius (decreasing salt concentration). For the large values of the Debye screening length far from a crossover point, a parameter λ_1 is a universal function of the Debye screening length and is almost independent of the initial value of the chain's bending energy, K. It is impossible to say what exactly happens with these two bending rigidities close to a crossover point because the error in separating two length scales increases as the value of the Debye radius decreases. Below we will develop a theoretical model, which describes this behavior of chain's bending rigidity.

3. Theoretical Model of Electrostatic Bending Rigidity

Consider a semiflexible chain with number of bonds, N, bond length, b, and fraction of charged monomers, α. Chain conformations are described by a set of the unit vectors $\vec{n}_i$ pointing along the chain bonds. The potential energy of a semiflexible polyelectrolyte chain with the bending energy, $k_B T K$, in a given conformation includes the bending energy and the electrostatic energy contributions

$$\frac{U_{PE}(\{\vec{n}_i\})}{k_B T} = \frac{K}{2}\sum_{i=0}^{N-2}(\vec{n}_i - \vec{n}_{i+1})^2 + \frac{l_B\alpha^2}{2}\sum_{i\neq j}^{N}\frac{\exp(-\kappa r_{ij})}{r_{ij}} \quad (7)$$

where r_{ij} is the distance between monomers i and j on the polymer backbone. In evaluating the contribution of electrostatic interactions, we will assume that a radius vector between monomers i and j along the polymer backbone does not deviate much from a straight line within the range of the exponential decay of the electrostatic potential. This

allows us to expand the distance between two monomers as follows

$$r_{ij} = b\sqrt{\left(\sum_{s=i}^{j-1}\vec{n}_s\right)^2} \approx bl_{ij}\left(1 - \left(\frac{1}{4l_{ij}^2}\sum_{s,s'}(\vec{n}_s - \vec{n}_{s'})^2\right)\right) \quad (8)$$

where $l_{ij} = |j - i|$ is the number of bonds between the ith and jth monomers along the polymer backbone. Using eq 8, we can expand the electrostatic potential energy about a rodlike conformation and obtain a correction to the electrostatic energy of a rod

$$\frac{\Delta U_{elec}(\{\vec{n}_i\})}{k_B T} \approx \frac{u\alpha^2}{4}\sum_{i<j}^{N}\frac{\exp(-\kappa bl_{ij})}{l_{ij}^3}(1+\kappa bl_{ij})\left(\sum_{s,s'=i}^{j-1}(\vec{n}_s - \vec{n}_{s'})^2\right) \quad (9)$$

where u is the ratio of the Bjerrum length, l_B, to the bond size, b. Therefore, the energy of a semiflexible polyelectrolyte chain in a given configuration depends only on the difference between the bond vectors. The partition function of a semiflexible polyelectrolyte chain is

$$Z = \int d\{\vec{n}_i\}\exp\left(-\frac{U_{PE}(\{\vec{n}_i\})}{k_B T}\right) \quad (10)$$

where integration in eq 10 is performed over all orientations of the unit vectors $\vec{n}_i$.

3.1. High-Temperature Expansion. Our simulations show that the electrostatic interactions between monomers lead to additional stiffening of a polyelectrolyte chain. Let us first calculate a correction to the chain bending rigidity by using a high-temperature expansion and evaluate the average value of $(\vec{n}_0 - \vec{n}_{N-1})^2$. For simplicity, we will assume that the initial chain bending rigidity, K, is large such that $K > N$. In this approximation, the electrostatic correction to the chain's energy in a given configuration is small, and we can expand the exponential function in powers of $\Delta U_{elec}(\{\vec{n}_i\})/k_B T$. This results in

$$\langle(\vec{n}_0 - \vec{n}_{N-1})^2\rangle = \frac{\langle(\vec{n}_0 - \vec{n}_{N-1})^2(1 - \Delta U_{elec}(\{\vec{n}_i\})/k_B T)\rangle_0}{\langle(1 - \Delta U_{elec}(\{\vec{n}_i\})/k_B T)\rangle_0} \quad (11)$$

where brackets $\langle\rangle_0$ denote the averaging with the statistical weight $\exp(-K\sum_{i=0}^{N-2}(\vec{n}_i - \vec{n}_{i+1})^2/2)$. The calculations of averages in eq 11 are straightforward if one introduces a new set of 2D vectors, $\vec{\tau}_i = \vec{n}_{i+1} - \vec{n}_i$, to describe a chain conformation. It is interesting to point out that the average $\langle(\vec{n}_0 - \vec{n}_{N-1})^2\rangle$ can be considered as a mean-square average value of the "end-to-end" vector of the effective 2D chain with conformations described by the bond vectors, $\vec{\tau}_i$. Because the vectors $\vec{\tau}_i$ and $\vec{\tau}_j$ are uncorrelated for a neutral semiflexible chain, we obtain $\langle(\vec{n}_0 - \vec{n}_{N-1})^2\rangle_0 = 2(N-1)/K$. Using correlation properties of the vectors $\vec{\tau}_i$ and after some algebra, we can rewrite eq 11 in the following form

$$\langle(\vec{n}_0 - \vec{n}_{N-1})^2\rangle \approx \left(\frac{2N}{K} - \frac{2}{3}\frac{N^2}{K^2}\frac{u\alpha^2}{\kappa b} - \frac{N}{2K^2}\frac{u\alpha^2}{(\kappa b)^2}\right)\left(1 - \frac{N}{3K}\frac{u\alpha^2}{\kappa b}\right)^{-1} \quad (12)$$

In simplifying the last equation, we have assumed that $N \gg 1$ and $\kappa b \ll 1$. If the electrostatic corrections are small, then one can assume that the electrostatic interactions renormalize the value of the bending constant such that $\langle (\vec{n}_0 - \vec{n}_{N-1})^2 \rangle \approx 2N/\lambda$, with $\lambda = K + \Delta K$. Solving eq 12 for the parameter λ, we obtain

$$\Delta K \approx \frac{u\alpha^2}{4(\kappa b)^2} \quad \text{and} \quad \lambda \approx K + \frac{u\alpha^2}{4(\kappa b)^2} \tag{13}$$

Therefore, the high-temperature expansion leads to an OSF-like correction to the chain's bending energy.[9,10] The advantage of the presented above approach is that it does not use any assumption about a trial chain conformation, as was done in the original OSF calculations.[9,10]

3.2. Mode Analysis. To calculate the correlation function between two bond vectors separated by l bonds along the polymer backbone in the case of an arbitrary N and K, we will introduce the normal coordinates for a set of the bond vectors $\{\vec{n}_i\}$

$$\vec{n}_s = \vec{a}_0 + 2 \sum_{k=1}^{N-1} \vec{a}_k \cos\left(\frac{\pi k s}{N}\right) \tag{14}$$

In this representation, the mode dependent part of the chain's potential energy is a quadratic function of the mode amplitudes

$$\frac{\Delta U_{PE}(\{\vec{a}_k\})}{k_B T} = N \sum_{k=1}^{N-1} \left(K\left(\frac{k\pi}{N}\right)^2 + V\left(\frac{k\pi}{N}\right) \right) \vec{a}_k^2 \tag{15}$$

where we defined

$$V(q) = 2u\alpha^2 \sum_{m=1}^{N} \left(1 - \frac{m}{N}\right) \frac{\exp(-\kappa b m)}{m^3} (1 + \kappa b m)$$
$$\left(\sum_{s=1}^{m} (m-s)(1 - \cos(qs)) \right) \tag{16}$$

We can perform summation over variable s in the rhs of eq 16 explicitly $(m^2 - (1 - \cos(mq))/(1 - \cos(q)))/2$, however it is useful to keep the summation over s in eq 16 because it simplifies calculations of the integrals. (See discussion below and Appendix A.) In normal mode representation, the bond−bond correlation function $G(l)$ describing the decay of the orientational memory along the polymer backbone

$$G(l) = \frac{1}{N-l} \sum_{s=0}^{N-l-1} \langle (\vec{n}_s \cdot \vec{n}_{s+l}) \rangle \tag{17}$$

is equal to

$$G(l) = \langle \vec{a}_0^2 \rangle + 2 \sum_{k=1}^{N-1} \langle \vec{a}_k^2 \rangle \cos\left(\frac{k\pi l}{N}\right) \tag{18}$$

Before proceeding further, let us point out that normal modes are not independent. It follows from observation that a value of the bond−bond correlation function, $G(0)$, should be equal to unity, which imposes a constraint on the mode spectrum

$$1 = \langle \vec{a}_0^2 \rangle + 2 \sum_{k=1}^{N-1} \langle \vec{a}_k^2 \rangle \tag{19}$$

To account for this constraint, we will introduce a Lagrange multiplier, μ, and modify the expression for the chain's potential energy as follows

$$\frac{\Delta U_{PE}(\{\vec{a}_k\}, \mu)}{k_B T} = N \sum_{k=1}^{N-1} \left(K\left(\frac{k\pi}{N}\right)^2 + V\left(\frac{k\pi}{N}\right) + \mu \right) \vec{a}_k^2 + \frac{N\mu \vec{a}_0^2}{2} \tag{20}$$

The value of the parameter μ should be found self-consistently from eq 19. Note that the mode analysis of a semiflexible polyelectrolyte chain in a continuous limit was also done by Barrat and Joanny.[11] The main difference between the two approaches is the introduction of the Lagrange multiplier to maintain normalization of the bond vectors.

The chain's potential energy is a quadratic function of the mode amplitudes and thus the averaging over the modes reduces to calculation of the Gaussian integrals. After some algebra, we have

$$1 = \frac{2}{\pi} \int_0^\infty \frac{dq}{Kq^2 + V(q) + \mu} \tag{21}$$

In rewriting eq 19, we have introduced $q = k\pi/N$ and substituted summation by integration. In the case of the neutral chain, $V(q) = 0$, the integral in the rhs of the eq 20 is easily evaluated, resulting in $\mu = 1/K$. In the case of the weak electrostatic interactions, we can expand the integrand in a power series of $V(q)$.

$$1 \approx \frac{2}{\pi} \int_0^\infty \frac{dq}{Kq^2 + \mu} - \frac{2}{\pi} \int_0^\infty \frac{V(q)\, dq}{(Kq^2 + \mu)^2} \tag{22}$$

Equation 22 is a self-consistent equation for determining the parameter, μ. Performing integration over q, we obtain

$$1 = \frac{1}{\sqrt{\mu K}} - \frac{u\alpha^2}{\sqrt{\mu^3 K}} g(\mu, K) \tag{23}$$

where we introduced

$$g(\mu, K) = \sum_{m=1}^{N} \left(1 - \frac{m}{N}\right) \frac{\exp(-\kappa b m)}{m^3} (1 + \kappa b m)$$
$$\sum_{s=1}^{m} (m-s) \left(1 - \left(1 + \sqrt{\frac{\mu}{K}} s\right) \exp\left(-\sqrt{\frac{\mu}{K}} s\right) \right) \tag{24}$$

The summation in eq 24 can be performed analytically for the large values of the parameter $K\kappa b \gg 1$. In this case, the exponential function $\exp(-s(\mu/K)^{1/2})$ can be approximated by its power series. In the framework of this approximation, the function $g(\mu, K) \approx \mu/(8K(\kappa b)^2)$. Assuming that electrostatic interactions are weak (high-temperature expansion) and result in a small correction to the parameter μ in comparison with the case of a neutral chain such that it can be approximated by $\mu^{-1} = K + \Delta K$, we can solve eq 23 for ΔK to obtain

$$\Delta K \approx \frac{u\alpha^2}{4(\kappa b)^2} \quad \text{and} \quad \mu \approx \left(K + \frac{u\alpha^2}{4(\kappa b)^2}\right)^{-1} \tag{25}$$

Knowing the value of the parameter μ, we can calculate a bond−bond correlation function

$$G(l) = \frac{2}{\pi} \int_0^\infty \frac{\cos(ql)\,\mathrm{d}q}{Kq^2 + V(q) + \mu} \approx \frac{2}{\pi} \int_0^\infty \frac{\cos(ql)\,\mathrm{d}q}{Kq^2 + \mu} \\ - \frac{2}{\pi} \int_0^\infty \frac{V(q)\cos(ql)\,\mathrm{d}q}{(Kq^2 + \mu)^2} \tag{26}$$

The exact expression for the bond−bond correlation function is complicated, but it has a relatively simple form for the length scales smaller than the chain persistence length bK, $l/K \ll 1$. In this approximation, the bond−bond correlation function is equal to

$$G(l) \approx 1 - \frac{l}{K} + \frac{u\alpha^2}{3K^2} \sum_{m=1}^{N} \left(1 - \frac{m}{N}\right) \frac{\exp(-\kappa bm)}{m^3} \\ (1 + \kappa bm) \sum_{s=1}^{m} (m-s) \begin{cases} l^2(3s-l), & l \le s \\ s^2(3l-s), & s \le l \end{cases} \tag{27}$$

The analysis of eq 27 shows that there are two different asymptotic regimes in the dependence of the bond−bond correlation function on the distance, l, along the polymer backbone. At the distances along the polymer backbone smaller than the reduced Debye screening length, $l\kappa b < 1$, the electrostatic correction shows quadratic dependence on the distance between monomers, l, such that

$$G(l) \approx 1 - \frac{l}{K} + \frac{u\alpha^2 l^2}{3K^2\kappa b} \approx 1 - \frac{l}{K + \frac{u\alpha^2 l}{3\kappa b}} \quad \text{for} \quad l\kappa b < 1 \tag{28a}$$

However, at the distances larger than the reduced Debye screening length, the leading term in the expansion is linear in l

$$G(l) \approx 1 - \frac{l}{K} + \frac{u\alpha^2 l}{4K^2(\kappa b)^2} \approx 1 - \frac{l}{K + \frac{u\alpha^2}{4(\kappa b)^2}} \quad \text{for} \\ l\kappa b > 1 \tag{28b}$$

Therefore, the effective chain persistence length is scale-dependent. At short distances, the electrostatic correction to the chain bending rigidity scales linearly with the value of the Debye screening length, whereas at large distances along the polymer backbone, it shows the OSF-like quadratic dependence.[9,10] One can write down a simple crossover expression for the scale-dependent chain's bending rigidity, $K(l)$, which will cover both asymptotic regimes

$$K(l) \approx K + \frac{u\alpha^2 l}{\kappa b(3 + 4\kappa bl)} \tag{29}$$

It is interesting to point out that the scale dependence of the chain bending rigidity could lead to a weaker than quadratic dependence of the chain persistence length on the Debye screening length. Another point worth making here is that the electrostatic corrections to the chain bending energy for $l = 1$ reproduce the result obtained in refs 19 and 20 using a Gibbs−Bogoulubov variational principle. This indicates that a variational principle based on the renormalization of the chain's bending constant can correctly describe the chain's properties only at distances smaller than the Debye screening length and fails to account for the additional chain stiffening at the larger distances. However, the OSF calculations[9,10] neglect high-frequency
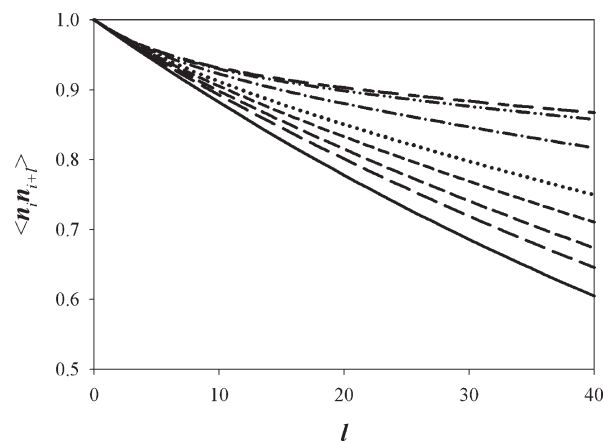

Figure 3. Theoretically calculated bond−bond correlation functions of semiflexible polyelectrolyte chains with the degree of polymerization, $N_\mathrm{m} = 200$, electrostatic coupling constant, $A_\mathrm{el} = 1.0$, bending constant, $K = 80.0$, and different values of the Debye screening length. The bond−bond correlation function of a neutral chain is shown by a solid line. Notations are the same as in Figure 1.
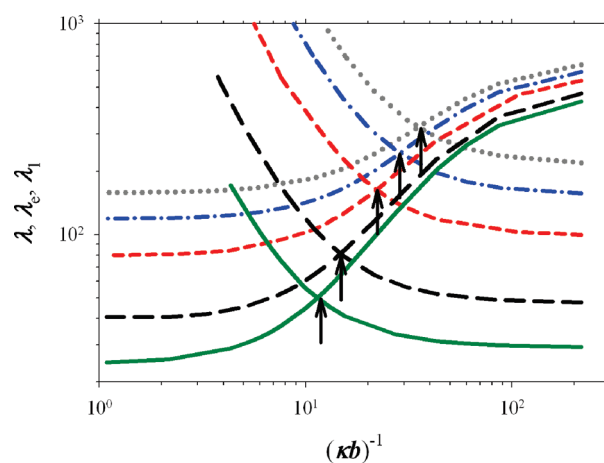

Figure 4. Dependence of the bending rigidities λ, λ_e, and λ_1 on the Debye screening length obtained from numerically calculated bond−bond correlation functions for semiflexible polyelectrolyte chains with the degree of polymerization, $N_\mathrm{m} = 200$, electrostatic coupling constant, $A_\mathrm{el} = 1.0$, and with different bending constants, $K = 25.0$ (green solid line), $K = 40.0$ (long dashed line), $K = 80.0$ (red short dashed line), $K = 120.0$ (blue dashed−dotted line), and $K = 160.0$ (gray dotted line). Arrows show intersection points between λ_1 and λ_e.

chain deformation modes, which control the chain bending rigidity at distances shorter than the Debye screening length.

To verify the validity of our approach in Figure 3, we show the results of numerical integration of the eq 26 with the value of the parameters μ determined from eq 21. The numerically calculated bond−bond correlation functions show behavior similar to those observed in our simulations. The agreement between simulation results and numerical calculations is good. The difference between the two does not exceed 5%. In Figure 4, we used our numerically calculated bond−bond correlation function to obtain dependence of the parameters λ, λ_1, and λ_e on the Debye screening length. Whereas there is obvious qualitative similarity between the Figures 2 and 4, the numerically evaluated effective bending rigidities are always lower than those obtained from simulations. Therefore, expression eq 26 underestimates the effect of the electrostatic interactions on renormalization of the chain's bending rigidities. Also, the agreement between numerically evaluated parameters

and simulation results worsens as the initial chain's bending rigidity decreases.

3.3. Variational Approach. To understand the reason behind the change of the form of the bond−bond correlation function, we will evaluate the integral in eq 21 by using a trial function approach. The form of the trial function can be established by analyzing the dependence of the function $V(q)$ on the wavenumber, q. In the limit $q\kappa b \ll 1$, this function is quadratic on q, $V(q) \propto q^2$, whereas in the opposite limit, $q\kappa b \gg 1$, it approaches a constant, $V(q) \propto \ln(\kappa b)$. Therefore, we can approximate function $V(q)$ by a trial function in the following form

$$V_{tr}(q) = \frac{Aq^2}{\delta^2 + q^2} \tag{30}$$

where parameters A and δ should be found self-consistently from the following equation

$$1 = \frac{2}{\pi}\int_0^\infty \frac{dq}{G^{-1}(q)} - \frac{2}{\pi}\int_0^\infty \frac{(V(q) - V_{tr}(q))\, dq}{[G^{-1}(q)]^2} \tag{31}$$

where we introduced the bond−bond correlation function in q representation

$$G^{-1}(q) = Kq^2 + \frac{Aq^2}{\delta^2 + q^2} + \mu \tag{32}$$

Note that our trial correlation function, eq 32, is different from that used in refs 15 and 16, where it was assumed that $\delta = \kappa b$. Because function $G^{-1}(q)$ represents a bond−bond correlation function, the first integral in the rhs of eq 31 should be equal to unity to satisfy the normalization condition for the norm of the unit vector. Therefore, eq 31 represents two independent conditions

$$1 = \frac{2}{\pi}\int_0^\infty \frac{dq}{G^{-1}(q)} \quad \text{and} \quad \frac{2}{\pi}\int_0^\infty \frac{(V(q) - V_{tr}(q))\, dq}{[G^{-1}(q)]^2} = 0 \tag{33}$$

where the first equation determines μ as a function of the parameters K, A, and δ, whereas the second one provides the relation between A and δ and system parameters K, $u\alpha^2$, and κb. Note, that the values of the parameters A and δ satisfying eqs 33 minimize the difference between functions $V(q)$ and $V_{tr}(q)$. In this respect, one can consider eqs 33 to be an analogue of the Edwards−Singh variational principle for the function $V(q)$.

To evaluate the integrals in eqs 33, it is useful to rewrite function $G(q)$ in the following form

$$G(q) = \frac{1}{K(z_2^2 - z_1^2)}\left[\frac{\delta^2 - z_1^2}{q^2 + z_1^2} + \frac{z_2^2 - \delta^2}{q^2 + z_2^2}\right] \tag{34}$$

where z_1 and z_2 are roots of the equation

$$z^4 - (\delta^2 + \mu/K + A/K)z^2 + \mu\delta^2/K = 0 \tag{35}$$

Note that the product of the roots is $z_1^2 z_2^2 = \mu\delta^2/K$. Analyses of the solutions of eq 35 shows that the roots of the eq 35 can be approximated by

$$z_1^2 = \frac{\mu}{K^*}, \quad z_2^2 = \frac{\delta^2 K^*}{K}, \quad K^* \approx K + \frac{A+\mu}{\delta^2} \tag{36}$$

Substitution of the function $G(q)$, given by eq 34, into the first integral of eq 33 leads to

$$1 = \frac{\delta\sqrt{K} + \sqrt{\mu}}{K(z_1 + z_2)\sqrt{\mu}} \approx \frac{\delta}{z_2\sqrt{K\mu}} \Rightarrow \mu \approx (K^*)^{-1} \tag{37}$$

The evaluation of the integrals in the second condition, eq 33, requires some persistence. The calculation details and numerical solution of eq 33 are given in Appendix A; here we will provide a qualitative analysis of these equations

$$K^*\left(\frac{u\alpha^2}{8(\kappa b)^2} - \frac{A}{2\delta^2}\right) + \frac{\Delta K}{\delta^3}\left(\frac{u\alpha^2(\Delta K - 4K)}{2K^{*3/2}K^{1/2}}\ln((\kappa b)^{-1})\right.$$
$$\left. + \frac{4u\alpha^2}{3\kappa b}\frac{\delta}{K^*} - \frac{A}{2\sqrt{K^* K}}\right) = 0 \tag{38}$$

where $\Delta K = K^* - K$. To satisfy the last equation, both terms in the brackets should simultaneously be equal to zero. This results in

$$\frac{u\alpha^2}{4(\kappa b)^2} = \frac{A}{\delta^2} \tag{39}$$

Therefore, a parameter δ is a solution of the following quadratic equation

$$\frac{u\alpha^2(\Delta K - 4K)}{2K^*}\ln((\kappa b)^{-1}) + \frac{4u\alpha^2}{3\kappa b}\sqrt{\frac{K}{K^*}}\delta - \frac{\Delta K}{2}\delta^2 = 0 \tag{40}$$

The solution of eq 40 has a simple form in two limiting cases. We will first consider the case, $K^* - K \approx K$. In this approximation, we have to balance the first and the last terms in eq 40

$$\delta^2\sqrt{\frac{K^*}{K}} \approx -u\alpha^2\frac{1}{\sqrt{K^* K}}\ln(\kappa b) \Rightarrow \delta^2 \approx -\frac{u\alpha^2}{K^*}\ln(\kappa b) \tag{41}$$

This leads to the following expression for the roots of the equation

$$z_1 = 1/K^* \quad \text{and} \quad z_2 = \delta\sqrt{K^*/K} \approx \sqrt{-\frac{u\alpha^2}{K}\ln(\kappa b)} \tag{42}$$

It also shows that $K^* \approx K + \frac{u\alpha^2}{4(\kappa b)^2}$.

In the other limit, $K^* - K \approx K$, the second and the third terms in eq 40 determine the value of the parameter δ

$$\delta \approx \frac{8}{3}\frac{u\alpha^2}{\kappa b \Delta K}\sqrt{\frac{K}{K^*}} \propto \kappa b \tag{43}$$

In this asymptotic regime, a value of the parameter δ is proportional to the inverse Debye screening length, κb. This is similar to the result obtained in refs 15 and 16. A crossover between two regimes takes place at a value of the Debye screening length

$$(\kappa b)_{cr} \propto \left(\frac{u\alpha^2}{K}\right)^{1/2} \tag{44}$$

The results of the numerical solution of the eqs 33 are given in Appendix A.

The bond−bond correlation function corresponding to the trial function $G(q)$, given by eq 32, is equal to

$$G(l) = (1 - \beta) \exp(-z_1|l|) + \beta \exp(-z_2|l|) \quad (45)$$

where parameter β is defined as

$$\beta = \frac{z_2^2 - \delta^2}{K(z_2^2 - z_1^2)z_2} \approx \frac{\Delta K}{\delta K^{*3/2} K^{1/2}} \quad (46)$$

The correlation function, eq 45, has a form similar to the one observed in our simulations if one substitutes $\lambda_1 = 1/z_1$ and $\lambda_2 = 1/z_2$. Our analysis of the bond−bond correlation function showed that the value of the parameter $\lambda_1 \approx K^* \approx K + u\alpha^2/4(\kappa b)^2$ coincides with the OSF expression for the chain's bending rigidity in the presence of the electrostatic interactions. The new feature in comparison with the OSF result is the existence of the second length scale characterized by parameter λ_2. It is worth pointing out that at low salt concentrations (large values of the Debye radius), the dependence of $\lambda_2^{-1} = z_2 \approx (-u\alpha^2 \ln(\kappa b)/K)^{1/2}$ on the system parameters coincides with that of a semiflexible chain with the bending rigidity, K, under tension with the external force $fb/k_B T = -u\alpha^2 \ln(\kappa b)$. Therefore, at short distances, electrostatic interactions lead to local chain deformation, which is manifested in the initial fast decay of the correlation function, $G(l)$. However, for small values of the Debye screening lengths, the contribution of the second exponential function is negligible at the distances along the polymer backbone larger than the Debye screening length, $\lambda_2 \propto (\kappa b)^{-1}$. (See Appendix A.) One can associate this exponential term with the high frequency modes that control the chain's bending rigidity at short-length scales. It is important to point out that our variational principle shows the existence of two length scales in the bond−bond correlation function throughout the entire salt concentration range. However, it is difficult to identify the second exponential function at high salt concentrations (small values of the Debye screening length) in simulations because of the small value of the parameter β. (See Figures 2 and 4.)

In Figure 5, we tested a scaling dependence of the parameter $\Delta K \propto u\alpha^2/(\kappa b)^2 = A_{el}\sigma^3/((\kappa\sigma)^2 b^3)$ on the reduced value of the Debye screening length, $A_{el}^{1/2}(\kappa\sigma)^{-1}$. Indeed, the simulation data follow the expected scaling dependence. The solid line in Figure 5 has a slope of 2. The deviation of the simulation data from the power law occurs when the value of the Debye screening length becomes comparable to the chain's contour length, Nb. This is a manifestation of the finite chain length effect. Note that in our simulations, the average bond length changes with increasing strength of the electrostatic interactions. (See Appendix B.) To account for this effect, the effective value of the bond length, b, was evaluated for each value of the Debye screening length. To compare our simulations with the experimental data, we have also added the data points for salt dependence of the DNA persistence length.[5] Further confirmation of the validity of our explanation of the shape change of the bond−bond correlation function comes from Figure 6. In this Figure, we plotted the dependence of the reduced value of the amplitude of the second exponential function, $\beta(A_{el}K\sigma/b)^{1/2}$, on the effective reduced temperature, $(A_{el}\sigma/Kb(\kappa b)^2)^{1/2}$. Note that the value of the amplitude, β, approaches zero for the values of the Debye screening length below a crossover value. (See eq 44.) This choice of the reduced parameters allowed us to collapse all of our simulation data into one master curve.
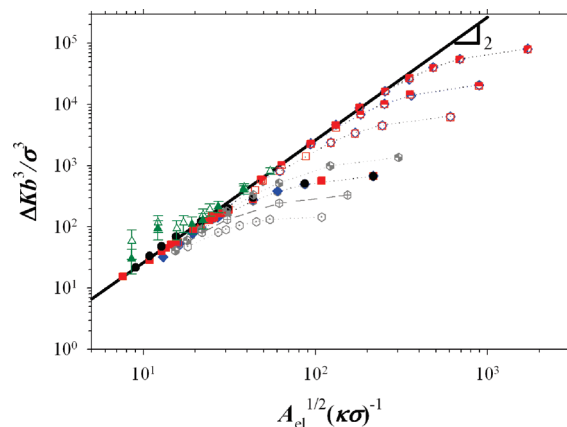

Figure 5. Dependence of the parameter $\Delta K b^3/\sigma^3$ on the parameter $A_{el}^{1/2}(\kappa\sigma)^{-1}$ for semiflexible polyelectrolyte chains with the degree of polymerization, $N_m = 200$, bending constants, $K = 40.0$ (circles), $K = 80.0$ (squares), $K = 120.0$ (rhombs), and $K = 160.0$ (hexagons), with electrostatic coupling constants, $A_{el} = 0.25$ (open symbols with dot), $A_{el} = 0.5$ (open symbols with cross), $A_{el} = 1.0$ (filled symbols), $A_{el} = 2.0$ (checkered symbols), $A_{el} = 9.0$ (open symbols), $A_{el} = 25.0$ (top filled symbols), and $A_{el} = 100.0$ (left filled symbols). The solid line is the best fit given by the equation $\Delta K b^3/\sigma^3 = 0.264 A_{el}(\kappa\sigma)^{-1}$. The experimental data for DNA from Hagerman[5] are shown as open triangles for 587 bp and filled triangles for 434 bp. We obtained the value of the parameter $A_{el} = 0.093$ for the experimental data by assuming the distance between effective charges $b = 0.17$ nm (an effective projection length between charges), degree of ionization $\alpha = 0.15$, and value of the Bjerrum length $l_B = 0.7$ nm.
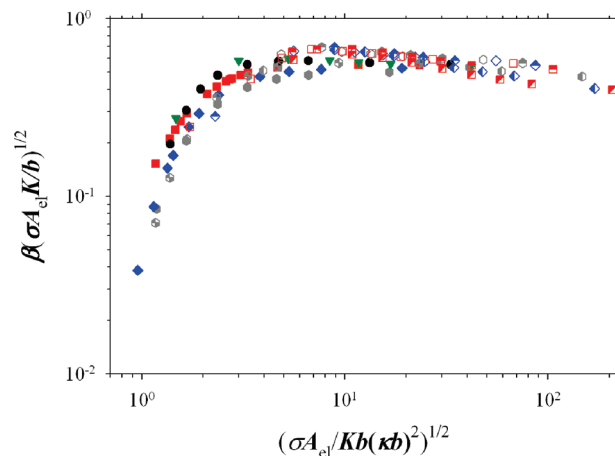

Figure 6. Dependence of the parameter $\beta(A_{el}K\sigma/b)^{1/2}$ on the parameter $(A_{el}\sigma/Kb(\kappa b)^2)^{1/2}$ for semiflexible polyelectrolyte chains with the degree of polymerization, $N_m = 200$, with bending constants, $K = 40.0$ (circles), $K = 80.0$ (squares), $K = 120.0$ (rhombs), and $K = 160.0$ (hexagons), with electrostatic coupling constants, $A_{el} = 1.0$ (filled symbols), $A_{el} = 2.0$ (checkered symbols), $A_{el} = 9.0$ (open symbols), $A_{el} = 25.0$ (top filled symbols), and $A_{el} = 100.0$ (left filled symbols).

4. Conclusions

Molecular dynamics simulations and theoretical calculations have shown that the electrostatic-induced stiffening of biological (semiflexible) polyelectrolytes is a multiscale process. A bond−bond correlation function of a polyelectrolyte chain can be approximated by a sum of two exponential functions, indicating the existence of two characteristic length scales (long-length scale and short-length scale correlation lengths) that control the chain's orientational memory. The long-length scale correlation length determines a decay of the orientational memory between bonds separated by distances along the polymer backbone larger than the Debye screening length. On this length scale, the chain's effective bending rigidity is a quadratic function of the Debye

screening length. The short-length scale correlation length scales linearly with the Debye screening length at high salt concentrations. However, at low salt concentrations, $\kappa b < ((u\alpha^2)/K)^{1/2}$, electrostatic interactions between charged monomers lead to weak (logarithmic) renormalization of the chain's bending constant. In this concentration range, local chain bending properties are similar to those of a semiflexible chain under electrostatic tension. Let us estimate the typical salt concentrations at which such a crossover may occur, $(\kappa b)_{cr} \propto ((u\alpha^2)/K)^{1/2}$. Below, we will assume that the fraction α of charged monomers on the polymer backbone is set at the Manning–Oosawa counterion condensation value $\alpha \approx b/l_B$.[11,12,21] This condition determines a low bound on the distance between ionized groups along the polymer backbone. Taking this into account, we can rewrite a crossover condition in terms of the chain's persistence length and solution Bjerrum length, $(\kappa^{-1})_{cr} \approx 1/(l_p l_B)^{1/2}$. For a DNA molecule in water at room temperature with the value of the Bjerrum length, $l_B = 7$ Å, and persistence length, $l_p \approx 50$ nm, a crossover takes place at ionic strengths on the order of $I \approx 2.5 \times 10^{-3}$ M, which is below a biologically relevant range of the ionic strengths, $I \approx 0.1$ to 0.01 M. However, it is possible to observe this crossover in solutions of synthetic polyelectrolytes or single stranded DNA, for which typical values of the persistence length are about 50 times shorter, $l_p \approx 10$ A. In this case, a crossover value of the ionic strength is about $I \approx 10^{-1}$ M. For lower solution ionic strengths (or larger Debye screening lengths), we predict that a short-length scale bond–bond correlation function has a form characteristic of a semiflexible chain under tension. The experimental verification of our results could be done by measuring a force–extension curve of a polyelectrolyte chain that probes the effect of the electrostatic interactions on the chain's elasticity on different length scales. We hope that this article will inspire experimental studies to test our model.

It is important to point out that the total effect of the electrostatic interactions on the chain's conformations is reduced to the local chain stiffening, which is manifested in the renormalization of the chain's persistence length and to the additional chain swelling, which is due to interactions between remote along the polymer backbone charges. Until now, we have assumed that the electrostatic interactions only influence the local chain's properties, such as its bending rigidity. This is usually true for relatively short chains or high salt concentrations when the contribution of the electrostatic interactions between remote along the polymer backbone charged pairs is small. These interactions become important at salt concentrations or chain degree of polymerizations for which the value of the Fixman interaction parameter $(B_{el} N^{1/2})/(b^3 \lambda_1^{3/2})$ (where B_{el} is the electrostatic second virial coefficient), is larger than unity.[22] The detailed analysis of the swelling effects on the chain's properties is presented in our recent article.[23]

Another point worth making here is that a two-scale form of the bond–bond correlation function should also be expected for flexible polyelectrolytes. Indeed, it has already been observed in simulations of flexible polyelectrolytes.[24−26] It would be nice if the authors reanalyze their simulation data by using our model. A study in this direction could highlight common features in the behavior of flexible and semiflexible polyelectrolytes.

Appendix A

In this Appendix, we will present the calculation details of the evaluation of the integrals in eq 33 and present numerical solutions for the variational parameters. We begin with the calculation of the second integral in eq 33 to obtain a self-consistent equation coupling the variational parameters μ, A, and δ with the system parameters

$$\frac{2}{\pi} \int_0^\infty \frac{(V(q) - V_{tr}(q))\, dq}{[G^{-1}(q)]^2} = 0 \tag{A1}$$

where

$$V(q) = 2u\alpha^2 \sum_{m=1}^N \left(1 - \frac{m}{N}\right) \frac{\exp(-\kappa bm)}{m^3}(1 + \kappa bm) \left(\sum_{s=1}^m (m-s)(1 - \cos(qs))\right) \tag{A2}$$

$$V_{tr}(q) = \frac{Aq^2}{\delta^2 + q^2} \tag{A3}$$

and

$$G(q) = \frac{1}{K(z_2^2 - z_1^2)}\left[\frac{\delta^2 - z_1^2}{q^2 + z_1^2} + \frac{z_2^2 - \delta^2}{q^2 + z_2^2}\right] \tag{A4}$$

The integration in eq A1 can be performed analytically resulting in

$$
\begin{aligned}
0 = \frac{1}{K^2(z_2^2 - z_1^2)^2} [& (\delta^2 - z_1^2)^2 I_1(z_1) + (\delta^2 - z_2^2)^2 I_1(z_2) \\
& + (\delta^2 - z_1^2)(z_2^2 - \delta^2) I_2(z_1, z_2) - (\delta^2 - z_1^2)^2 g_3(z_1) \\
& - (\delta^2 - z_2^2)^2 g_3(z_2) - (\delta^2 - z_1^2)(z_2^2 - \delta^2) g_4(z_1, z_2) \\
& - (\delta^2 - z_1^2)^2 g_5(z_1) - (\delta^2 - z_2^2)^2 g_5(z_2) \\
& - (\delta^2 - z_1^2)(z_2^2 - \delta^2) g_6(z_1, z_2, \delta)]
\end{aligned}
\tag{A5}
$$

where we introduced

$$I_1(z) = 2u\alpha^2 \sum_{m=1}^N T(m) \sum_{s=1}^m (m-s) g_1(s, z) \tag{A6}$$

$$I_2(z_1, z_2) = 2u\alpha^2 \sum_{m=1}^N T(m) \sum_{s=1}^m (m-s) g_2(s, z_1, z_2) \tag{A7}$$

$$T(m) = \left(1 - \frac{m}{N}\right)\frac{\exp(-\kappa bm)}{m^3}(1 + \kappa bm) \tag{A8}$$

$$g_1(s, z) = \frac{2}{\pi}\int_0^\infty \frac{(1 - \cos(qs))}{(q^2 + z^2)^2}\, dq = \frac{1}{2z^3}(1 - (1 + sz)\exp(-sz)) \tag{A9}$$

$$
\begin{aligned}
g_2(s, z_1, z_2) &= \frac{4}{\pi}\int_0^\infty \frac{(1 - \cos(qs))}{(q^2 + z_1^2)(q^2 + z_2^2)}\, dq \\
&= \frac{2}{(z_2^2 - z_1^2)}\left(\frac{1 - \exp(-sz_1)}{z_1} - \frac{1 - \exp(-sz_2)}{z_2}\right)
\end{aligned}
\tag{A10}
$$

$$g_3(z) = \frac{2A}{\pi} \int_0^\infty \frac{dq}{(q^2+z^2)^2} = \frac{A}{2z^3} \qquad (A11)$$

$$g_4(z_1,z_2) = \frac{4A}{\pi} \int_0^\infty \frac{dq}{(q^2+z_1^2)(q^2+z_2^2)} = \frac{2A}{(z_2+z_1)z_1z_2} \qquad (A12)$$

$$g_5(z,\delta) = -A\delta^2 \frac{2}{\pi} \int_0^\infty \frac{dq}{(q^2+z^2)^2(q^2+\delta^2)}$$

$$= -A\delta \frac{(\delta+2z)}{2z^3(\delta+z)^2} \qquad (A13)$$

$$g_6(z_1,z_2,\delta) = -A\delta^2 \frac{4}{\pi} \int_0^\infty \frac{dq}{(q^2+z_1^2)(q^2+z_2^2)(q^2+\delta^2)}$$

$$= -2A\delta \frac{(\delta+z_1+z_2)}{z_1z_2(z_1+z_2)(z_1+\delta)(z_2+\delta)} \qquad (A14)$$

Using expressions for the functions eqs A6–A14, we can write eq A5 as follows

$$0 = \frac{1}{K^2(z_2^2-z_1^2)^2}\left[\left((\delta^2-z_1^2)^2 I_1(z_1) - \frac{A}{2}\frac{(\delta-z_1)^2}{z_1}\right)\right.$$

$$+(z_2^2-\delta^2)^2 I_1(z_2) + (\delta^2-z_1^2)(z_2^2-\delta^2)I_2(z_1,z_2) \qquad (A15)$$

$$\left. -\frac{A}{2}\left(\frac{(z_2-\delta)^2}{z_2} + 4\frac{(\delta-z_1)(z_2-\delta)}{z_1+z_2}\right)\right]$$

It is useful to introduce a new variable K^* such that

$$z_1^2 = \frac{\mu}{K^*}, \quad z_2^2 = \frac{\delta^2 K^*}{K}, \quad \frac{A}{\delta^2} = (K^*-K)\left(1-\frac{\mu}{K^*\delta^2}\right) \qquad (A16)$$

Using this new variable, we can transform eq A16 as follows

$$f_1(K^*,\mu,\delta) = \left(z_1 I_1(z_1) - \frac{(K^*-K)(1-y)}{2(1+y)}\right) = 0$$

$$f_2(K^*,\mu,\delta) = \left[\frac{(K^*-K)}{K(1-y^2)}z_2^2 I_1(z_2) + z_2^2 I_2(z_1,z_2)\right.$$

$$\left. -\frac{K^*\delta}{2}\left(\frac{(x-1)^2}{x} + 4\frac{(1-y)(x-1)}{x+y}\right)\right] = 0 \qquad (A17)$$

where we introduced reduced variables

$$x = \sqrt{\frac{K^*}{K}} = \frac{z_2}{\delta} \quad \text{and} \quad y = \frac{1}{\delta}\sqrt{\frac{\mu}{K^*}} = \frac{z_1}{\delta} \qquad (A18)$$

Equation A17 has to be supplemented by a normalization condition, eq 37

$$f_3(K^*,\mu,\delta) = 1 - \frac{1+xy}{(x+y)\sqrt{K\mu}} = 0 \qquad (A19)$$

The optimal values of the parameters K^*, μ, and δ can be found by minimizing a function

$$\chi(K^*,\mu,\delta) = f_1^2(K^*,\mu,\delta) + f_2^2(K^*,\mu,\delta) + f_3^2(K^*,\mu,\delta) \qquad (A20)$$

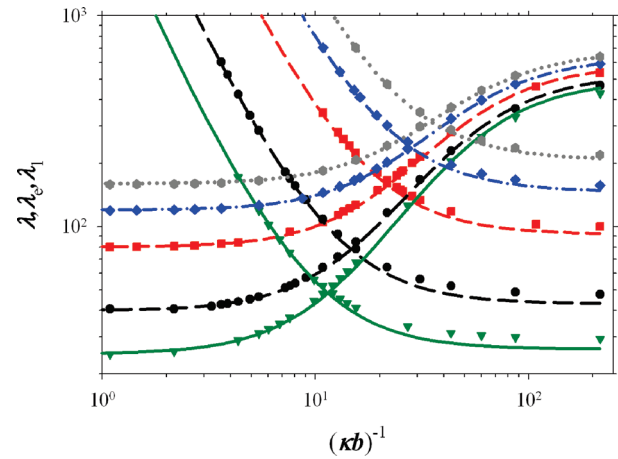**Figure 7.** Dependence of the bending rigidities λ, λ_e, and λ_1 on the Debye screening length obtained from numerically calculated bond–bond correlation functions (symbols) and from variational principle by solving system of eqs A17 and A19 (lines) for semiflexible polyelectrolyte chains with the degree of polymerization, $N_m = 200$, electrostatic coupling constant, $A_{el} = 1.0$, and with different bending constants, $K = 25.0$ (green solid line and triangles), $K = 40.0$ (black long-dashed line and circles), $K = 80.0$ (red short-dashed line and squares), $K = 120.0$ (blue dashed–dotted line and rhombs), and $K = 160.0$ (gray dotted line and hexagons).

Figure 7 shows the comparison between the bending rigidities obtained from the numerically calculated correlation functions, eq 26 (Figure 4), and those calculated from the variational approach by minimizing a χ function, eq A20. The agreement between the values of the bending rigidities is very good. The plots for the optimal value of the parameter δ are shown in Figure 8. The agreement between the direct integration results and the variational calculations is not as good as that for the bending rigidities. The difference between values of the parameter δ obtained by two methods increases with decreasing value of the Debye screening length. This supports our observation that it becomes more difficult to separate the two length scales at small values of the Debye radius.

Appendix B

In this appendix, we will describe a bond deformation with increasing strength of the electrostatic interactions. The free energy of the system with deformable bonds is

$$\frac{F(b,\mu)}{k_B T} \approx N U_{bond}(b)$$

$$+ u\alpha^2 \sum_{m=2}^N (N-m)\frac{\exp(-m\kappa b)}{m} \qquad (B1)$$

$$+ \sum_{q=0}^{N-1} \ln\left(K\left(\frac{q\pi}{N}\right)^2 + V\left(\frac{q\pi}{N}\right) + \mu\right) - \frac{\mu N}{2}$$

where the first term describes the bond energy with a bond length, b

$$U_{bond}(b) = -\frac{k_{spring}R_{max}^2}{2k_B T}\ln\left(1-\frac{b^2}{R_{max}^2}\right)$$

$$+ \frac{4\varepsilon_{LJ}}{k_B T}\left(\left(\frac{\sigma}{b}\right)^{12} - \left(\frac{\sigma}{b}\right)^6\right) + \frac{\varepsilon_{LJ}}{k_B T} \qquad (B2)$$

The functional form of this interaction potential corresponds to that used in our simulations. The second term in the rhs of
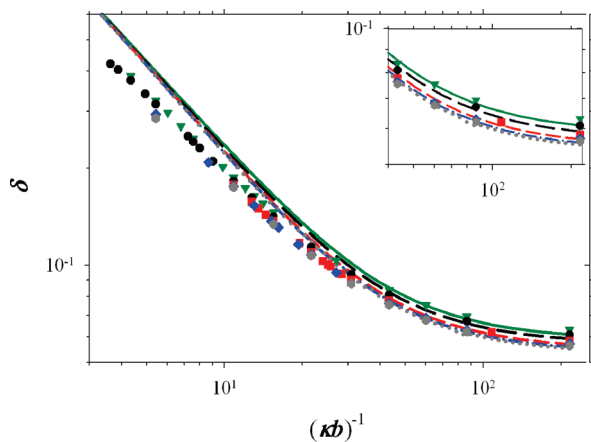
Figure 8. Dependence of the parameter δ on the Debye screening length obtained from numerically calculated bond−bond correlation functions (symbols) and from variational principle by solving system of eqs A17 and A19 (lines) of Appendix A for semiflexible polyelectrolyte chains with the degree of polymerization, $N_m = 200$, electrostatic coupling constant, $A_{el} = 1.0$, and with different bending constants, $K = 25.0$ (green solid line and triangles), $K = 40.0$ (black long-dashed line and circles), $K = 80.0$ (red short-dashed line and squares), $K = 120.0$ (blue dashed−dotted line and rhombs), and $K = 160.0$ (gray dotted line and hexagons).
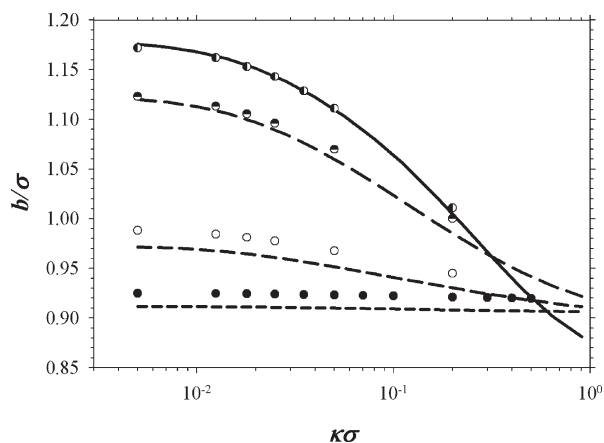

Figure 9. Equilibrium bond length, b, as a function of the Debye screening length for semiflexible polyelectrolyte chains with the degree of polymerization, $N_m = 200$, and with electrostatic coupling constants, $A_{el} = 1.0$ (filled symbols), $A_{el} = 9.0$ (open symbols), $A_{el} = 25.0$ (top filled symbols), and $A_{el} = 100.0$ (left filled symbols). Lines show equilibrium values of the bond length, b, obtained by solving eq B4 of Appendix B for different values of the electrostatic coupling constants $A_{el} = 1.0$ (short dashed line), $A_{el} = 9.0$ (medium dashed line), $A_{el} = 25.0$ (long dashed line), and $A_{el} = 100.0$ (solid line). The value of the spring constant was set to $k_{spring} = 90k_BT/\sigma^2$ for $A_{el} = 100.0$.

eq B1 describes the electrostatic interactions of a chain in the rodlike conformation with a bond length, b. (The summation in this expression starts with $m = 2$ because in our simulations, we have neglected 1−2 electrostatic interactions.) The logarithmic term in eq B1 accounts for orientational fluctuations of the bond vectors with respect to a rodlike conformation. Note that in writing eq B1, we have neglected terms that do not depend on the bond length, b, or the Lagrange multiplier, μ. The optimal values of the parameters b and μ are obtained by minimizing the free energy (eq B1). The optimization of the free energy, eq B1, with respect to the Lagrange multiplier, μ, reproduces eq 21

$$1 = \frac{2}{\pi} \int_0^\infty \frac{dq}{Kq^2 + V(q) + \mu} \tag{B3}$$

and optimization with respect to the bond length, b, results in

$$U'(b) + \frac{E'_{rod}(b)}{N} + \frac{1}{\pi} \int_0^\infty \frac{V'(q)\,dq}{(Kq^2 + V(q) + \mu)} = 0 \tag{B4}$$

where $f'(b)$ denotes the derivative of a function $f(b)$ with respect to the bond length, b, and we introduced $E_{rod}(b)$ for the electrostatic energy of a chain in a rodlike conformation (the second term in the rhs of eq B1). The results of the minimization procedure are summarized in Figure 9. The agreement between the simulation results and the numerical calculations improves with increasing strength of the electrostatic interactions.

References and Notes

(1) Bloomfield, V. A. DNA condensation by multivalent cations. *Biopolymers* **1997**, *44*, 269–282.
(2) Grosberg, A. Y.; Nguyen, T. T.; Shklovskii, B. I. Colloquium: The physics of charge inversion in chemical and biological systems. *Rev. Mod. Phys.* **2002**, *74*, 329–345.
(3) Levin, Y. Electrostatic correlations: from plasma to biology. *Rep. Prog. Phys.* **2002**, *65*, 1577–1632.
(4) Baumann, C. G.; Smith, S. B.; Bloomfield, V. A.; Bustamante, C. Ionic effects on the elasticity of single DNA molecules. *Proc. Natl. Acad. Sci. U.S.A.* **1997**, *94*, 6185–6190.
(5) Hagerman, P. J. Investigation of flexibility of DNA using transient electric birefringence. *Biopolymers* **1981**, *20*, 1503–1535.
(6) Hsieh, C. C.; Doyle, P. S. Studying confined polymers using single-molecule DNA experiments. *Korea-Aust. Rheol. J.* **2008**, *20*, 127–142.
(7) Han, J.; Craighead, H. G. Separation of long DNA molecules in a microfabricated entropic trap array. *Science* **2000**, *288*, 1026-1029.
(8) Jo, K.; Dhingra, D. M.; Odijk, T.; de Pablo, J. J.; Graham, M. D.; Runnheim, R.; Forrest, D.; Schwartz, D. C. A single-molecule barcoding system using nanoslits for DNA analysis. *Proc. Natl. Acad. Sci. U.S.A.* **2007**, *104*, 2673–2678.
(9) Odijk, T. Polyelectrolytes near the rod limit. *J. Polym. Sci., Polym. Phys. Ed.* **1977**, *15*, 477–483.
(10) Skolnick, J.; Fixman, M. Electrostatic persistence length of a wormlike polyelectrolyte. *Macromolecules* **1977**, *10*, 944–948.
(11) Barrat, J. L.; Joanny, J. F. Theory of polyelectrolyte solutions. *Adv. Chem. Phys.* **1996**, *94*, 1–66.
(12) Dobrynin, A. V.; Rubinstein, M. Theory of polyelectrolytes in solutions and at surfaces. *Prog. Polym. Sci.* **2005**, *30*, 1049–1118.
(13) Ullner, M. Comments on the scaling behavior of flexible polyelectrolytes within the Debye−Hückel approximation. *J. Phys. Chem. B* **2003**, *107*, 8097–8110.
(14) Dobrynin, A. V. Theory and simulations of charged polymers: from solution properties to polymeric nanomaterials. *Curr. Opin. Colloid Interface Sci.* **2008**, *13*, 376–388.
(15) Ha, B. Y.; Thirumala, D. Persistence length of flexible polyelectrolyte chains. *J. Chem. Phys.* **1999**, *110*, 7533–7541.
(16) Manghi, M.; Netz, R. R. Variational theory for a single polyelectrolyte chain revisited. *Eur. Phys. J. E* **2004**, *14*, 67–77.
(17) Frenkel, D.; Smit, B. *Understanding Molecular Simulations*; Academic Press: New York, 2002.
(18) Marko, J. F.; Siggia, E. D. Stretching DNA. *Macromolecules* **1995**, *28*, 8759–8770.
(19) Dobrynin, A. V. Electrostatic persistence length of semiflexible and flexible polyelectrolytes. *Macromolecules* **2005**, *38*, 9304–9314.
(20) Dobrynin, A. V. Effect of counterion condensation on rigidity of semiflexible polyelectrolytes. *Macromolecules* **2006**, *39*, 9519–9527.
(21) Manning, G. S. Counterion condensation theory constructed from different models. *Physica A* **1996**, *231*, 236–253.
(22) Doi, M.; Edwards, S. F. *The Theory of Polymer Dynamics*; Oxford University Press: New York, 1986.
(23) Dobrynin, A. V.; Carrillo, J.-M. Y. *Physica A* **2009**, in press.
(24) Micka, U.; Kremer, K. The persistence length of polyelectrolyte chains. *J. Phys.: Condens. Matter* **1996**, *8*, 9463–9470.
(25) Micka, U.; Kremer, K. Persistence length of weakly charged polyelectrolytes with variable intrinsic stiffness. *Europhys. Lett.* **1997**, *38*, 279–284.
(26) Nguyen, T. T.; Shklovskii, B. I. Persistence length of a polyelectrolyte in salty water: Monte Carlo study. *Phys. Rev. E* **2002**, *66*, 021801/1–7.